EuroGNC Navigation Guidance Control CEAS Bristol, UK June 11th-13th 2024
University of BRISTOL ROYAL AERONAUTICAL SOCIETY AIAA

Polynomial Range Impact Time Control: A Novel Approach Using Bézier Curves

Akın Çatak Istanbul Technical University, Aerospace Research Center, 34469, Istanbul, Turkey. catak15@itu.edu.tr

Esra Demir Istanbul Technical University, Aerospace Research Center, 34469, Istanbul, Turkey. demire15@itu.edu.tr

Raziye Tekin Roketsan Missiles Inc., Tactical Missile Systems, Ankara, Turkey. razytekin@gmail.com

Emre Koyuncu Istanbul Technical University, Aerospace Research Center, 34469, Istanbul, Turkey. emre.koyuncu@itu.edu.tr

İbrahim Özkol Istanbul Technical University, Aerospace Research Center, 34469, Istanbul, Turkey. ozkol@itu.edu.tr

ABSTRACT

Control over a missile's total flight time offers significant strategic advantages in military operations, including timed target engagement and orchestrated salvo attacks to boost success rates. To this end, this study introduces an innovative impact time guidance law tailored explicitly for planar engagement contexts, utilizing Bézier curves to shape the missile's range trajectory. A 4th-degree range curve is presented, from which a generalized form of the range polynomial is derived. Remarkably, our proposed guidance law aligns seamlessly with existing state-of-the-art impact time control guidance laws, thereby substantiating the efficacy and adaptability of Bézier curves in guidance law design. This alignment confirms the robust capabilities of Bézier curves as a design tool and opens new avenues for future research in developing increasingly complex and efficient guidance laws.

Keywords: Bézier curves; impact time guidance; polynomial range formulation

Nomenclature

V	=	magnitude of the missile velocity
a	=	normal acceleration of the missile
σ	=	look angle of the missile
λ	=	LOS angle
r	=	range
$\dot{\gamma}$	=	guidance command
t_f, t_{go}, t	=	desired impact time, remaining time to go, elapsed time
P_i	=	control points
Q_i	=	derivative curve control points

$B_{i,n}$ = basis functions
u = knot parameter
n = degree of the Bézier curve

1 Introduction

The significance of timed and angled coordinated attacks cannot be overstated in both traditional and unconventional combat scenarios, as they elevate potency and operational efficiency. These tactics enable an array of projectiles, missiles, or combat units to strike a target nearly simultaneously but from various vectors. This coordinated strike can incapacitate enemy defensive measures by giving them a narrow reaction time frame. Yet, executing such attacks presents immense challenges. Achieving the level of timing and synchronization needed among different units is a complex feat, often contingent upon split-second or minute angular adjustments. Additionally, real-time computational assessments must be made, considering numerous variables such as velocity, range, and even unpredictable target movements. Given the multifaceted nature of these variables, developing an effective strategy for such attacks remains an area of ongoing research.

The work [1] derived an impact time guidance law by decomposing the acceleration into two parts. This approach reduces the miss distance and achieves the required trajectory lengths. Although the performance of this guidance law is satisfactory, the time-to-go assumption in the proposed work is not desired. Several other works are solving the impact time problem while suffering from the same t_{go} estimation, i.e., [2], [3], and [4] which are using nonlinear control methods, Lyapunov formulation and modified version of pure proportional navigation respectively. In the literature, impact time guidance laws which do not utilize t_{go} estimation are also present [5], [6], [7], [8], and [9]. The works [5] and [6] have the same monotonically decreasing look angle magnitudes. At the same time, the first one solves the impact time problem using the Lyapunov formulation, and the second uses time-varying navigation gain for Proportional Navigation. The works [7], [8], and [6] solved the impact time problem using polynomial shaping methods for guidance variables such as range and look angle. Range is shaped as 4^{th} order polynomial in [7] and the general form of range polynomial is presented in closed loop form in [8]. This work deals with constraints in the look angle value as well as application domain problems such as autopilot lag and measurement noises. The work [6] solves the impact time problem in a similar manner yet shapes the look angle as a polynomial.

The guidance variables are not only shaped using analytical polynomials. Bézier curves, parametric polynomials, for shaping the range polynomial is used in [10] to obtain an open loop guidance law capable of ensuring impact time and angle constraints. The work utilizes the Feedback Linearization method and a numerical root-finding algorithm to completely shape the curve. The impact time and angle problem is solved using Bézier curves in [11]. This work proposes a four-stage guidance law. The first and second stages adjust the impact angle and heading angle, respectively. The third stage is responsible for tracking two segment trajectories. The terminal stage is the well-known PNG for reducing the miss distance. Bézier spirals and Differential Flatness are used in [12] to deal with impact time and angle problems. Trajectory length is formulated as a function of curvature to track the reference trajectory using differential flatness. The [13] investigates the impact time and angle problem by utilizing t_{go} estimation. The method in this paper consists of two stages. The first stage, the deployment stage, reduces the expected time to go error from the terminal stage, which is in the form of biased proportional navigation. The impact time and angle problem is solved in [14] by shaping the line of sight as 4^{th} order polynomial using Bézier curves. The complete shape of the LOS polynomial is obtained by an offline procedure. An optimization-based impact time guidance law with the help of the Bézier curve is proposed in [15]. The method shapes the range as a Bézier curve being at least 7^{th} degree. The reasoning behind this is the degree of freedom needed for the constraints. The method proposes three objective functions: the first

one is the total control effort, the second one is maximum acceleration, and the last one is the maximum look angle value. After the offline optimization finds a solution the open loop guidance command is created for impact time control.

This study aims to address the intricate problem of impact time control in missile guidance by leveraging the capabilities of Bézier curves with the motivation of finding stand-alone guidance laws rather than numerical routines, which may not be desirable for application purposes. The primary reason behind the selection of the Bézier curve is twofold: Bézier curves offer unparalleled control over the trajectory while providing a streamlined design and implementation process. The unique contribution of this research lies in elucidating the simplicity and effectiveness of employing Bézier curves in the design phases of any guidance law. To substantiate this, we derive an impact time guidance law for stationary targets along with its generalized form. Remarkably, our proposed guidance law and its broader application align closely with the state-of-the-art guidance laws as delineated in existing literature, specifically referenced [8]. By demonstrating this alignment, we aim to significantly advance the field, providing a more facile yet robust approach to tackling the complexities of impact time and angle control in missile systems.

The rest of the paper is organized as follows: The next section defines the planar engagement dynamics and formulates the impact time problem. Then Bézier formulation and its properties that will be used in this work are given. Guidance law design is divided into two sections. The latter one is for generalized range polynomials. Before the conclusion part, simulations are prepared to show the results of the proposed methodology as well as the comparison study with [15].

2 Methodology

For scenarios in which the target is assumed to be stationary, the planar engagement geometry is as shown in Fig. 1. Where M is the missile, V is the missile velocity, a is the normal acceleration of the

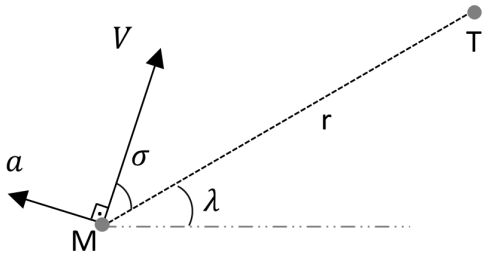

Fig. 1 2D engagement geometry when the target is stationary

missile, r is the range between the missile and the target, σ is the look angle, and λ is the line of sight (LOS) angle. The target is shown as T, and in this case, it is assumed to be stationary. The dynamic equations representing this geometry are as given in Eqs. (1) and (2).

$$\begin{aligned} \dot{r} &= -V\cos(\sigma) \\ \dot{\lambda} &= -\frac{V}{r}\sin(\sigma) \end{aligned} \tag{1}$$

$$\gamma = \lambda + \sigma \tag{2}$$

Obtaining the guidance command $\dot{\gamma} = a/V$ is called guidance law design. Designing guidance commands with different steps can give useful capabilities to the guidance law in addition to capturing the target. The particular impact time constraint for a guidance law can be described as completing the engagement within the prescribed time frame.

In other words, the missile should hit the target with a specified impact time, t_{des}. Additionally, for the stationary target, the look angle value at the terminal instant, σ_f, should be converging to zero in order to obtain zero miss distance.

To obtain an impact time guidance law, the first derivative of the range curve given in Eq. (1) is taken to get Eq. (3).

$$\begin{aligned} \ddot{r} &= V \sin\sigma \cdot \dot{\sigma} \\ \dot{\sigma} &= \frac{\ddot{r}}{V \sin\sigma} \end{aligned} \tag{3}$$

This function gives the rate of change of look angle σ. Using the derivative of Eq. (2) and combining it with the expression Eq. (3), guidance command is obtained for stationary targets as Eq. (4).

$$\begin{aligned} \dot{\sigma} &= \frac{\ddot{r}}{-\dot{\lambda} \cdot r} \\ \dot{\gamma} &= \dot{\lambda} + \dot{\sigma} \\ \dot{\gamma} &= \dot{\lambda} - \frac{\ddot{r}}{\dot{\lambda} r} \end{aligned} \tag{4}$$

This guidance law depends on the second derivative of the range curve and is capable of adjusting the terminal time constraints in a very wide range if the range polynomial is shaped as a function of time. The proceeding subsections will propose a suitable approach for range shaping.

2.1 Bézier Curve Integration

Bézier curves are mathematical representations characterized by parametric polynomials. They enable the shaping of a curve through the manipulation of so-called control points using their linear combinations, a process dependent on the curve's degree. Beyond the starting and ending points that the curve traverses, it relies on intermediate control points and their associated basis functions to construct the entire polynomial curve. The mathematical expression for a Bézier curve of degree n is detailed in Eq. (5). Further insights and details can be explored in the source reference [16].

$$C(u) = \sum_{i=0}^{n} B_{i,n}(u) P_i \quad 0 \le u \le 1 \tag{5}$$

In Eq. (5), n represents the degree of the curve, P_i corresponds to the i^{th} control point out of a total of n+1 control points, $B_{i,n}$ denotes the basis function, specifically the Bernstein Polynomial, associated with the i^{th} control point P_i, and u serves as the knot parameter. The computation of the basis function mentioned in Eq. (5) is determined using the formula outlined in Eq. (6).

$$B_{i,n}(u) = \frac{n!}{i!(n-i)!} u^i (1-u)^{n-i} \tag{6}$$

Here, n represents the degree, and i signifies the index of each control point, similar to the previous equation. The primary role of basis functions is to determine the influence of each control point on the Bézier curves of degree n. As basis functions are dependent on the parameter u for a given n, the contributions from different sets of control points remain the same for a specified degree and knot value. Fig. 2 illustrates how the Bézier curve varies when using the same degree but different control points. Blue and red circles in Fig. 2 represent the set of control points, and similarly, blue and red curves are the corresponding curves determined from this set of control points. By observing Fig. 2 and examining the equation governing the basis functions, it becomes evident that Bézier curves cannot be modified locally because all basis functions have nonzero values at all knot positions.

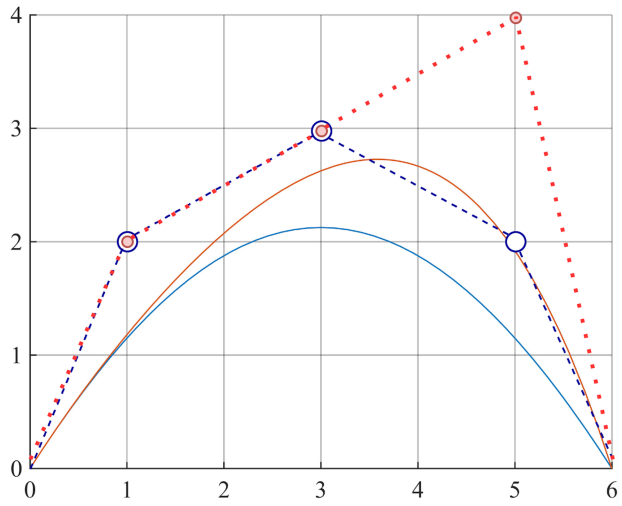

Fig. 2 4th degree Bézier curve and the effect of control point location

The derivative of any Bézier curve can be expressed using the control points of the original curve and basis functions of degree n-1. The relation for derivative curve control points and original curve control points, as well as the parametric equation for the derivative curve, are given in Eq. (7). For higher-order derivatives, you can iterate Eq. (7) up to the $(n-1)^{th}$ derivative, treating the derived curve as a new original curve, and so forth.

$$\begin{aligned} Q_i &= n(P_{i+1} - P_i) \\ C'(u) &= \sum_{i=0}^{n-1} B_{i,n-1}(u) Q_i \end{aligned} \tag{7}$$

where $C'(u)$ represents the derivative of the original curve with respect to u, n is the degree of original Bézier curve, Q_i denotes the control points of the derivative curve, and P_i signifies the control points of the original curve

In this study, initially, a fourth-degree Bézier curve and its second derivative have been employed. The previously mentioned observation that basis functions remain consistent for all potential curves of a given degree led to the formulation of Eqs. (8) and (9), which describe the fourth-degree Bézier curve and its corresponding second derivative, respectively. The general form of a Bézier curve in the polynomial form is given in section 4.2.

$$C(u) = (1-u)^4 P_0 + 4(1-u)^3 u P_1 + 6(1-u)^2 u^2 P_2 + 4(1-u) u^3 P_3 + u^4 P_4 \tag{8}$$

$$\frac{d^2 C(u)}{du^2} = 12(1-u)^2 (P_0 - 2P_1 + P_2) + 24(1-u)u (P_1 - 2P_2 + P_3) + 12u^2 (P_2 - 2P_3 + P_4) \tag{9}$$

2.2 Fourth Degree Range Polynomials

The range polynomial has at least two boundary conditions. Initial and final $\dot{r}$ values are needed to shape the curve. Additional $\ddot{r}$ at the final time is optional but preferred in order to achieve less change in the range polynomial at the final part of the engagement. For these reasons, 4^{th} degree Bézier curve is chosen as the polynomial shaping method. The boundary conditions determine the complete curve by

determining the locations of the control points P_i and derivative curve control points Q_i in Eq. (10).

$$\begin{aligned} P_0 &= r_0 \\ P_4 &= P_f = 0 \\ Q_0 &= \dot{r}_0 = -V\cos(\sigma_0) \\ Q_2 &= \dot{r}_f = -V\cos(\sigma_f) = -V \\ Q_3 &= Q_2 = -V \end{aligned} \tag{10}$$

The equality of $Q_3 = Q_2$ comes from the $\ddot{r}_f = 0$ condition. The initial and final conditions dictate the first and last control points P_0 and P_4 of the Bézier curve in Eq. (10). The remaining control points are determined by using the derivative control points Q_0, Q_2, and Q_3 coming from Eq. (10) using Eq. (13). Before diving into the determination of the remaining control points, the time parameterizing function borrowed from [10] is introduced in Eq. (11).

$$t = \frac{u}{\mu}, \qquad t \in [0, t_{go}] \tag{11}$$

where, $\mu = 1/t_{go}$ and t_{go} is the time to go term. Throughout the engagement, the remaining flight time decreases. Thus, as suggested in [8], the remaining time to go should be represented as the difference between designated impact time t_f and elapsed time t as in Eq.(12).

$$t_{go} = t_f - t \tag{12}$$

Designated impact time is fixed throughout the flight, whereas the time-to-go value changes with time. The following equations exploit the use of t_{go}, which is not estimated but found using Eq.(12).

$$\begin{aligned} P_1 &= P_0 + \left(\frac{t_{go}}{n}\right) Q_0 \\ P_2 &= P_3 - \left(\frac{t_{go}}{n}\right) Q_2 \\ P_3 &= P_f - \left(\frac{t_{go}}{n}\right) Q_3 \end{aligned} \tag{13}$$

The guidance command in Eq. (4) requires the $\ddot{r}_0$ value at each time step. This value can be found using the following Eq. (14).

$$\ddot{r}_0 = \frac{n}{t_{go}} (Q_1 - Q_0) \tag{14}$$

The expression Q_1 is found using the following Eq. (15).

$$Q_1 = \frac{n}{t_{go}} (P_2 - P_1) \tag{15}$$

Additionally, there is an analytical expression that can be obtained for the guidance law presented. The derivation steps for closed-form guidance law start with Eq. (9).

$$\begin{aligned} \ddot{r}(0) t_{go}^2 =& 12(1-0)^2 (P_0 - 2P_1 + P_2) + 24(1-0)0 (P_1 - 2P_2 + P_3) \\ &+ 12(0^2) (P_2 - 2P_3 + P_4) \end{aligned} \tag{16}$$

Then, simply substitute all the control points into the Eq. (16) to obtain the final expression.

$$\ddot{r}(0)t_{go}^2 = 12\left(P_0 - 2\left(P_0 + \left(\frac{t_{go}}{4}\right)Q_0\right) + \left(P_3 - \left(\frac{t_{go}}{4}\right)Q_2\right)\right) \tag{17}$$

$$\ddot{r}(0)t_{go}^2 = 12\left(r_0 - 2\left(r_0 + \left(\frac{t_{go}}{4}\right)\dot{r}_0\right) + \left(\left(r_f - \left(\frac{t_{go}}{4}\right)\dot{r}_3\right) - \left(\frac{t_{go}}{4}\right)\dot{r}_2\right)\right) \tag{18}$$

Substituting the derivative control points yields the following equation,

$$\begin{aligned}\ddot{r}(0)t_{go}^2 =& 12\left(r_0 - 2\left(r_0 + \left(\frac{t_{go}}{4}\right)(-V\cos(\sigma_0))\right)\right) \\ &+ 12\left(\left(0 + \left(\frac{t_{go}}{4}\right)V\right) + \left(\frac{t_{go}}{4}\right)V\right)\end{aligned} \tag{19}$$

Rearranging the Eq. (19) and substituting the control point P_0 gives the Eq. (20)

$$\ddot{r}(0)t_{go}^2 = -12r_0 + 6Vt_{go}\cos(\sigma_0) + 6Vt_{go} \tag{20}$$

$$\ddot{r}(0) = \frac{-12r_0 + 6Vt_{go}\cos(\sigma_0) + 6Vt_{go}}{t_{go}^2} \tag{21}$$

The guidance law can be derived using the analytical form of $\ddot{r}$ in Eq. (21). The Eq. (23) is the impact time control guidance law obtained using Bézier curve approach.

$$\begin{aligned}\dot{\gamma} &= \dot{\lambda} - \frac{\ddot{r}}{\dot{\lambda}r} \\ \dot{\gamma} &= \dot{\lambda} + \frac{-12r_0 + 6Vt_{go}\cos(\sigma_0) + 6Vt_{go}}{V\sin(\sigma_0)\,t_{go}^2}\end{aligned} \tag{22}$$

The transition between r_0 to r is possible since the current value of the range can be thought of as the initial range value for the designed Bézier curve. The same applies to σ as well.

$$\dot{\gamma} = \dot{\lambda} + \frac{-12r + 6Vt_{go}(1 + \cos(\sigma))}{V\sin(\sigma)\,t_{go}^2} \tag{23}$$

The t_f expression in Eq. (23) represents the remaining time to go for each time step. Note that the Eq. (23) is the same as the equation 20 in [7]. The reason behind this result is the same initial and final constraints for the same polynomial degree. This result demonstrates the possible usage of Bézier curves as proper guidance law derivation tools.

2.3 Generalized Range Polynomials

Let's give n^{th} degree Bézier curve formulation.

$$r_n(u) = (1-u)^n P_0 + nu(1-u)^{n-1}P_1 + \ldots + nu^{n-1}(1-u)P_{n-1} + u^n P_n \tag{24}$$

Note that the control points P_i and derivative curve control points Q_i have a relation for Bézier curves as in the following equation,

$$P_i = P_{i-1} + \frac{t_{go}}{n}Q_{i-1} \tag{25}$$

Keeping this relation in mind and assigning $Q_{(n-1,n-2,n-3...,2)} = -Vcos(\sigma_f) = -V$ should define the complete n^{th} degree Bézier curve. The guidance command derived in Eq. (4) use the $\ddot{r}(0)$ value. Thus, the second derivative of the curve in Eq. (24) is simplified as in Eq. (26)

$$\ddot{r}_n(0)t_{go}^2 = n(n-1)(P_0 - 2P_1 + P_2) \tag{26}$$

The value of the control point P_0 is the range value for each step. P_1 and P_2 can be found using boundary conditions and the t_{go} is the remaining time to go term. The equations defining the P_1 and P_2 is given in Eqs. (27) and (28) respectively.

$$P_1 = P_0 + \frac{t_{go}}{n}Q_0 \tag{27}$$

where Q_0 is the same as in Eq. (10). The calculation of P_2 involves some repetitive calculation solving from the last control point to P_2.

$$\begin{aligned}
P_{n-1} &= P_n - \frac{t_{go}}{n}Q_{n-1} \\
P_{n-1} &= P_n + \frac{t_{go}}{n}V \\
P_{n-2} &= P_{n-1} - \frac{t_{go}}{n}Q_{n-2} \\
P_{n-2} &= P_{n-1} + \frac{t_{go}}{n}V \\
P_{n-2} &= P_n + 2\frac{t_{go}}{n}V \\
&\vdots \\
P_{n-m} &= P_n + m\frac{t_{go}}{n}V \\
&\vdots \\
P_2 &= P_n + (n-2)\frac{t_{go}}{n}V
\end{aligned} \tag{28}$$

Then the last part is to combine the Eqs. (26), (27), and (28) and substitute the resulting equation into the guidance law.

$$\begin{aligned}
\ddot{r}_n(0)t_{go}^2 &= n(n-1)(P_0 - 2(P_0 - \frac{t_{go}}{n}Vcos(\sigma_0) + (P_n + (n-2)\frac{t_{go}}{n}V)) \\
\ddot{r}_n(0)t_{go}^2 &= n(n-1)(-P_0 + 2\frac{t_{go}}{n}Vcos(\sigma_0) + (n-2)\frac{t_{go}}{n}V)
\end{aligned} \tag{29}$$

The resulting guidance law is given in Eq. (30)

$$\dot{\gamma} = \dot{\lambda} - \frac{\frac{n(n-1)(-P_0 + 2\frac{t_{go}}{n}Vcos(\sigma_0) + (n-2)\frac{t_{go}}{n}V)}{t_{go}^2}}{\dot{\lambda}r} \tag{30}$$

Rearranging the guidance law obtained for n^{th} degree range polynomial gives the following Eq. (31).

$$\dot{\gamma} = \dot{\lambda} + \frac{n(n-1)(-P_0 + 2\frac{t_{go}}{n}Vcos(\sigma_0) + (n-2)\frac{t_{go}}{n}V)}{Vsin(\sigma_0)t_{go}^2}$$
$$\dot{\gamma} = \dot{\lambda} + \frac{(n-1)(-nP_0 + (n-2+2cos(\sigma_0))t_{go}V)}{Vsin(\sigma_0)t_{go}^2} \tag{31}$$

For a closed loop guidance law, the obtained guidance law in Eq. (32)

$$\dot{\gamma} = \dot{\lambda} + \frac{2}{Vsin(\sigma)}\Delta \tag{32}$$

where Δ is,

$$\Delta = \frac{n-1}{2t_{go}^2}(-nr + (2cos(\sigma) + n - 2)t_{go}V) \tag{33}$$

The resulting guidance law in Eq. (32) is the same as in [8]. Additionally, taking the polynomial degree n as 4 leads to Eq. (23) as expected. Since there is $sin(\sigma)$ term in the denominator part of the Eq. (32) and Eq. (23), it will result in singularity when zero look angle is reached. This is indeed a typical case for stationary targets. The avoidance of this singularity is discussed in [8] for application purposes. However, it is not included in this study for the sake of simplicity. Slowly moving targets can be captured by a predicted impact point approach if the target has a constant known speed. The characteristic of the seeker is another issue to be addressed. Higher tf and n values will result in higher maximum look angle values in the engagements. Thus, if there is a field of view limitation for the seeker, some of the n and tf combinations may not be feasible.

3 Simulation and Comparison

In this section, the application of the guidance law described in this study is presented for 2 different scenarios. One of these scenarios is given with the same parameters as in [8] (Scenario 1), where the same guidance law is obtained, so that the results obtained can be validated. In the other scenario, an air-to-ground engagement is simulated using a different set of engagement parameters. In this scenario, different desired impact times have also been investigated. Results are given for $n = 4, 5$, and 6 in both scenarios. For all simulations, when the miss distance dropped below 5m, the target was considered to have been captured and the simulation was terminated. The parameters in the mentioned scenarios are provided in Table 1.

Table 1 Parameters of different scenarios

Parameters	Scenario 1	Scenario 2
$V(m/s)$	200	300
$t_f(s)$	35	25, 30, 60, 90
$\sigma_0(deg)$	15	30
$P_{Missile}(m)$	[0, 0]	[0, 2000]
$P_{Target}(m)$	[5000, 0]	[6000, 0]

Fig. 3 illustrates the implementation of scenario 1. In this figure, in addition to the reference paper [8], an application for $n = 6$ is also given, and an autopilot modeling as first-order lag with a time constant of $1s$ for this value is also added to the results, as well as $n = 4$ and 5. When the graphs in the figure are examined individually, looking at the Range and attitude-downrange graphs, it is seen that in all simulations, the missile reaches the target at the desired impact time. In the look angle graph, it can

be observed that the maximum look angle of the missile increases with the increase in n, while the case with autopilot has the maximum look angle. If the seeker's limit is 60 deg, then the only option is $n = 4$ for this scenario. When the acceleration graph is considered, it is clear that in the case where $n = 4$, the acceleration is not 0 at the end of the time the missile reaches the target, while in the other 3 cases, it reaches 0. It is also concluded that as n increases, the magnitude of the acceleration at the beginning of the flight also increases.

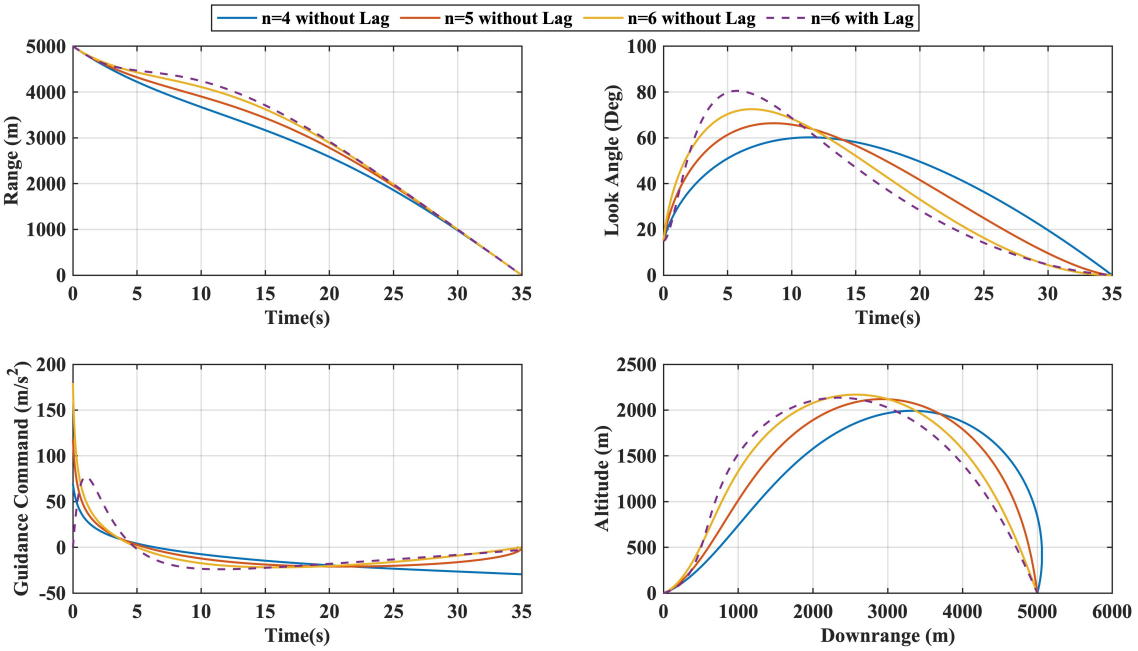

Fig. 3 Implementation of the scenario in the [8] for different values of n and autopilot effect for n=6

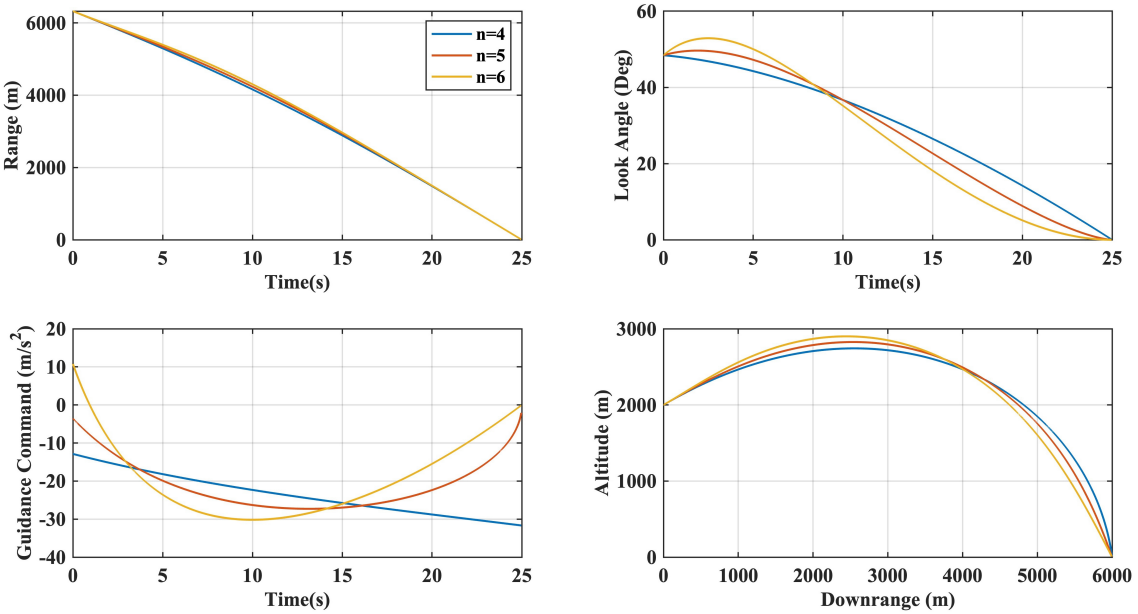

Fig. 4 Implementation of scenario 2 for different n values

Fig. 4 represents the implementation of scenario 2 for $n = 4, 5$, and 6. Looking at the range and attitude-downrange graphs in the figure, it is observed that for all n values, the target is impacted in the desired time. Looking at the look angle graph, similar to the previous scenario, it can be seen that the

maximum look angle of the missile increases with increasing n. However, at the end of the simulation for all cases, it is clear that the look angle is 0. Considering the guidance command graph, again, it is observed that for $n = 4$, the acceleration value of the missile at the moment of impact with the target is not 0. For the other two simulations, these values reach 0 at the end of the time. However, as n increases, the acceleration value at the beginning of the simulation increases.

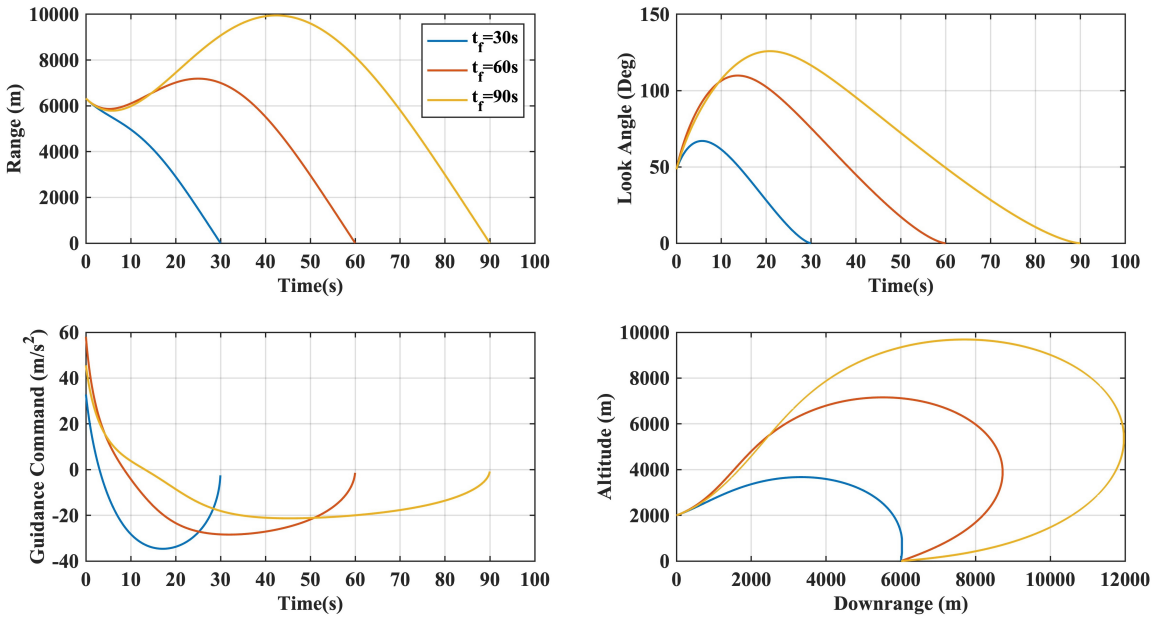

Fig. 5 Comparison of scenario 2 with different impact times t_f

Fig. 5 presents the plots analyzing different impact times using the parameters in scenario 2 and taking $n = 5$. In the range-time plot, it is clear that the target is successfully reached at the desired impact times. In the look angle-time plot, the maximum look angle of the missile increases with increasing impact time. The results are satisfactory for a simulation, but due to the field of view limits of the seeker, the higher impact times are not feasible in real-world scenarios. In the guidance command plot, the final acceleration reached 0 at impact instant for all time values. The initial acceleration increased with increasing t_f value.

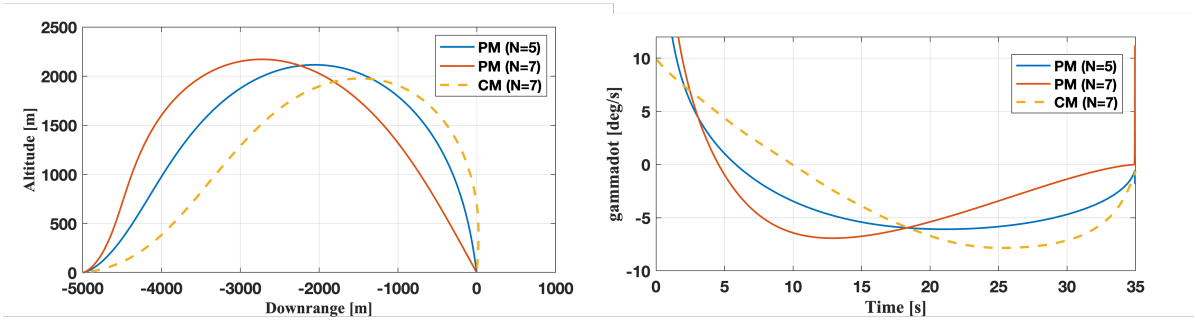

Fig. 6 Comparison of the proposed method and method presented in [15].

The proposed impact time guidance law is compared with the [15], stated as CM in Fig. 6, using their engagement conditions. The ground-to-ground engagement for stationary targets using two different Bézier curve degrees and the result of CM is given in Fig. 6. Both methods are capable of achieving desired impact time values, with trajectories being slightly different for each solution. The proposed method, stated as PM in Fig.6, demands more acceleration in the beginning due to the design choices made in the Bézier curve. This is due to the derivatives of range up to $n - 2$ being -V in the proposed

method. Although this has a positive result as the final acceleration demands are smaller and converge zero faster as the Bézier curve degree increases, it necessitates more acceleration demand at the beginning of the engagement. This results in a total control effort of $J = 0.02035$ for $n = 5$ and $J = 0.04265$ for $n = 7$ while comparing $J = 0.010435$ for the CM. If the maximum $\dot{\gamma}$ is limited to $10deg/s$, which is the maximum acceleration command of the CM, the cost of the PM for $n = 5$ drops to $J = 0.01064$, which is similar to the CM. Additionally, the offline algorithm presented in the CM can be affected more by the disturbance and the uncertainties since it does not have feedback to correct the deviations. Also, the lower terminal acceleration commands are welcomed in most scenarios to reduce the probability of missing the target.

4 Conclusion

In summary, this research introduces an impact time guidance law that leverages the potential of Bézier curves to shape the missile's range as a parametric function. Notably, our derived guidance law aligns seamlessly with one of the recognized state-of-the-art guidance laws from recent scholarly contributions, thereby underscoring the efficacy and versatility of Bézier curves as a tool for guidance law design. The successful implementation and alignment of our proposed model reinforce the promise of Bézier curves in this domain. Since the proposed method is an online analytical method and does not involve optimization, its feasibility is higher than offline methods or algorithms that include optimization. Although the given guidance law has satisfactory performance and can be used in a real system, it has some limitations and drawbacks. Two dimensional engagement dynamics and the stationary target assumption can be a limitation for some of the operations. The speed of the missile in a realistic scenario may not be constant and continuously changing due to the gravitational acceleration and drag force. Looking ahead, future studies will concentrate on these issues and the derivation of more intricate but not complex stand-alone guidance laws. Possible modifications to this guidance law may encompass both impact time and angle control, as well as collaborative guidance schemes for three-dimensional engagements under varying velocities. These advanced frameworks will also be grounded in Bézier curve formulations, extending the applicability and utility of this approach in addressing complex challenges in missile guidance and control.

References

[1] In-Soo Jeon, Jin-Ik Lee, and Min-Jea Tahk. Impact-time-control guidance law for anti-ship missiles. *IEEE Transactions on control systems technology*, 14(2):260–266, 2006.

[2] Dongsoo Cho, H Jin Kim, and Min-Jea Tahk. Nonsingular sliding mode guidance for impact time control. *Journal of Guidance, Control, and Dynamics*, 39(1):61–68, 2016.

[3] Mingu Kim, Bokyung Jung, Bumku Han, Sangchul Lee, and Youdan Kim. Lyapunov-based impact time control guidance laws against stationary targets. *IEEE Transactions on Aerospace and Electronic Systems*, 51(2):1111–1122, 2015.

[4] Namhoon Cho and Youdan Kim. Modified pure proportional navigation guidance law for impact time control. *Journal of Guidance, Control, and Dynamics*, 39(4):852–872, 2016.

[5] Abdul Saleem and Ashwini Ratnoo. Lyapunov-based guidance law for impact time control and simultaneous arrival. *Journal of Guidance, Control, and Dynamics*, 39(1):164–173, 2016.

[6] In-Soo Jeon and Jin-Ik Lee. Impact-time-control guidance law with constraints on seeker look angle. *IEEE Transactions on Aerospace and Electronic Systems*, 53(5):2621–2627, 2017.

[7] Raziye Tekin, Koray S Erer, and Florian Holzapfel. Quartic range shaping for impact time control. In *2017 25th Mediterranean Conference on Control and Automation (MED)*, pages 1213–1218. IEEE, 2017.

[8] Raziye Tekin, Koray S Erer, and Florian Holzapfel. Impact time control with generalized-polynomial range formulation. *Journal of Guidance, Control, and Dynamics*, 41(5):1190–1195, 2018.

[9] Raziye Tekin, Koray S Erer, and Florian Holzapfel. Polynomial shaping of the look angle for impact-time control. volume 40, pages 2668–2673. American Institute of Aeronautics and Astronautics, 2017.

[10] Suwon Lee and Youdan Kim. Optimal output trajectory shaping using bézier curves. *Journal of Guidance, Control, and Dynamics*, 44(5):1027–1035, 2021.

[11] Heng Shi, Zhiqiang Cheng, Minchi Kuang, Jihong Zhu, Xinghui Yan, and Xiangxiang Li. Four-stage guidance law for impact time and angle control based on the bezier curve. *IEEE Transactions on Aerospace and Electronic Systems*, 2023.

[12] Yiwei Wang, Ruichen Li, Zihao Wu, Kang Chen, and Dengxiu Yu. Precise impact time and angle guidance strategy under time-varying velocity. *Nonlinear Dynamics*, pages 1–17, 2024.

[13] Gun-Hee Moon, Sang-Wook Shim, and Min-Jea Tahk. Bezier-curve navigation guidance for impact time and angle control. *INCAS Bulletin*, 10(1):105–115, 2018.

[14] Akın Çatak and Emre Koyuncu. Dynamic line of sight shaping for impact time and angle control guidance. *IFAC-PapersOnLine*, 56(2):4514–4519, 2023.

[15] Suwon Lee and Raziye Tekin. Impact time control with bézier curves. In *CEAS EuroGNC 2022*, 2022.

[16] Les Piegl and Wayne Tiller. *The NURBS book*. Springer Science & Business Media, 1996.